

Load dependence of densification in glass during Vickers indentation test

Yoshinari KATO,^{*,**,†} Hiroki YAMAZAKI,^{*} Satoru ITAKURA,^{**} Satoshi YOSHIDA^{**} and Jun MATSUOKA^{**}

^{*}Technical Division, Nippon Electric Glass Co., Ltd., Otsu 520-8639

^{**}School of Engineering, The University of Shiga Prefecture, Hikone, Shiga 522-8533

The load dependence of densification during a Vickers indentation test was investigated for three commercial glass compositions, soda-lime silicate glass, aluminoborosilicate glass, and lead borosilicate glass, each of which exhibits markedly different susceptibility to crack initiation. The contribution of densification to the total deformation due to indentation was evaluated as the ratio of the depths of indentation before and after heat treatment measured with an atomic force microscope (AFM). For the soda-lime silicate and aluminoborosilicate glasses, the contribution of densification decreases with increasing applied load, but the rate of the decrease is less for the aluminoborosilicate glass than for the soda-lime silicate glass. For the lead borosilicate glass, the contribution of densification is low throughout the range of loads investigated. The residual stress can be estimated from the contribution of densification, and the variation of load dependence of the residual stress is considered to result in a large difference in the crack initiation load among the glasses.

©2011 The Ceramic Society of Japan. All rights reserved.

Key-words : Oxide glass, Crack initiation, Indentation, Residual stress

[Received October 14, 2010; Accepted November 26, 2010]

1. Introduction

Crack initiation and crack propagation are the most important factors determining the strength of glass. It is well known that glass exhibits a very high theoretical strength of close to 10 GPa. However, once a crack initiates in the glass surface, stress concentration occurs at the crack tip, resulting in catastrophic fracture even under an applied stress much lower than the theoretical strength. Thus, the evaluation of crack initiation and crack propagation is of considerable interest for glass engineers and glass scientists.

Crack propagation is usually evaluated by measuring fracture toughness, K_{IC} . Glass with higher K_{IC} has higher breaking strength for a given flaw size. Although various glass compositions have almost the same value of K_{IC} , there is a marked difference in the susceptibility to fracture among glasses in industrial and practical use. It is considered that this difference is due to a difference in crack initiation behavior. Therefore, the characteristics of both crack initiation and crack propagation must be evaluated to understand glass strength.

Unlike crack propagation which can be evaluated by measuring K_{IC} , a method of evaluating crack initiation of glass has not yet been established, although some methods have been proposed. Wada et al.¹⁾ proposed “crack resistance (CR)” of glass against Vickers indentation. When a glass sample is indented with a Vickers diamond indenter, radial cracks initiate around the indentation at a given indentation load. The value of CR is defined as the load required for the radial cracks to initiate, indicating the difficulty of crack initiation. On the other hand, Lawn and Marshall²⁾ proposed the ratio of hardness to fracture toughness as a simple index of brittleness, and it was reported that this “brittleness” index has a clear relationship with crack initiation behavior.³⁾ In addition, Sehgal et al.⁴⁾ developed a convenient method of estimating the “brittleness” index of glass

by using the ratio of the characteristic crack length to the length of the indentation diagonal.

In our previous study,⁵⁾ CR for various commercial glass compositions was investigated by using Vickers indentations, and CR values were compared with other mechanical properties. It was found that the value of CR does not have a clear relationship with general mechanical properties, such as K_{IC} and hardness, but it has a clear relationship with the recovery of indentation depth (RID). The value of RID is the ratio of the change in indentation depth due to heat treatment to the indentation depth before heat treatment, and it is a measure of the degree of densification occurring during indentation. Densification is an inelastic deformation that is accompanied by a change in volume. The value of CR increased with increasing RID in our previous study.⁵⁾ It was concluded that densification should reduce residual stress around the indentation, thus preventing cracks from initiating.

However, the difference in crack resistance among various glass compositions was much larger than that in the residual stress. **Figure 1** shows the relationship between crack resistance and the estimated residual stress around an indentation at a load of 100 gf.⁵⁾ The residual stress ranges over a factor of two (0.3 to 0.6 GPa) while CR ranges over a factor of about 30 (30 to 1300 gf). On the other hand, it was reported that soda-lime silicate glass exhibits a load-dependent contribution of densification to deformation.⁶⁾ Therefore, densification affects the residual stress, so the load dependence of the contribution of densification to deformation should affect cracking behavior during indentation. However, the load dependences of the contribution of densification for various commercial glasses have not been clarified.

In the present study, densification during indentation tests is evaluated at various loads using a dynamic hardness tester and an atomic force microscope, AFM, then the effect of the load dependence of the contribution of densification on crack resistance is discussed.

[†] Corresponding author: Y. Kato; E-mail: ykato@neg.co.jp

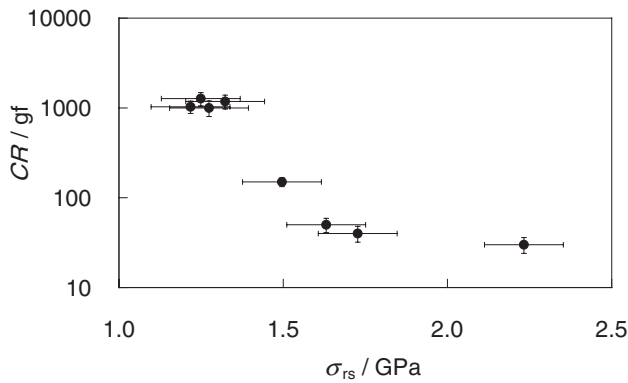


Fig. 1. Relationship between crack resistance, CR , and estimated residual stress around indentations when indented at a load of 100 gf.⁵⁾

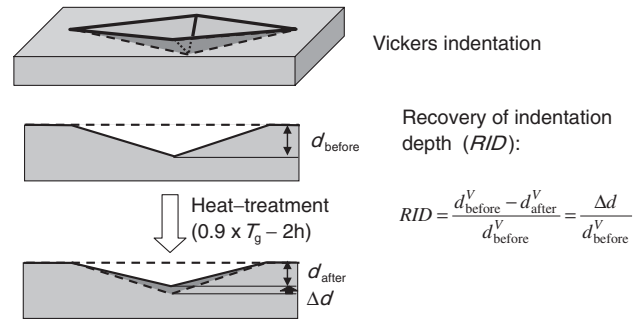


Fig. 2. Schematic of method used to measure recovery of indentation depth (RID).

Table 1. General compositions of glasses and their density (ρ), glass transition temperature (T_g), fracture toughness (K_{IC}), Young's modulus (E), bulk modulus (K), and crack resistance (CR)⁵⁾

Name	General composition (mol %)	ρ (g/cm ³)	T_g (°C)	K_{IC} (MPa·m ^{1/2})	E (GPa)	K (GPa)	CR (gf)
C	70SiO ₂ -10Al ₂ O ₃ -10B ₂ O ₃ -10Others	2.48	710	0.79	70	40	1200 (900-1400)
D	70SiO ₂ -10Na ₂ O-10CaO-10Others	2.49	540	0.75	72	40	150 (140-170)
G	60SiO ₂ -25PbO-5B ₂ O ₃ -10Others	4.44	470	0.66	63	44	30 (25-40)

Molar fractions of minor components in the glass composition are omitted.

Experimental uncertainties are as follows: d : ± 0.01 g/cm³ (Archimedes method), T_g : $\pm 2^\circ\text{C}$ (dilatometer method), K_{IC} : ± 0.05 MPa·m^{1/2} (SEPB method), E : ± 1 GPa (resonance method), and K : ± 1 GPa (resonance method)

2. Experimental

Among the glass compositions investigated in the previous study,⁵⁾ three glass compositions with markedly different values of CR were selected for the present study. The first is Glass C, aluminoborosilicate glass, whose crack resistance is 1200 gf. The second is Glass D, soda-lime silicate glass, whose crack resistance is 150 gf. The third is Glass G, lead borosilicate glass, whose crack resistance is 30 gf. The general compositions and properties of these glasses are shown in Table 1. The methods of measuring CR and the other properties are described in the previous paper.⁵⁾ Samples of the glasses were ground, lapped with Al₂O₃ slurry, and then finished with cerium oxide to obtain optically smooth surfaces, which were used in the following indentation test.

The contribution of densification to the total deformation due to indentation was evaluated by measuring the recovery of indentation depth after heat treatment.⁷⁻⁹⁾ The recovery is attributed to annealing recovery of densified glass under a high compressive stress.¹⁰⁾ The procedure for measuring the recovery of indentation depth is shown in Fig. 2. A glass sample was indented at various loads from 5 to 200 gf for 15 s using a Vickers indenter with a dynamic hardness tester (DUH-201, Shimadzu, Japan), and the diagonal and depth of the indentation were measured with an AFM (Nanoscope IIIa Digital Instruments, USA). The indented sample was heat-treated at a temperature of $0.9 \times T_g$ (in °C) for 2 h, and the indentation depth was measured again. The ratio of the change in depth to the depth before the heat treatment was defined as the recovery of indentation depth, RID , given by the following equation:

$$RID = (d_{\text{before}}^V - d_{\text{after}}^V) / d_{\text{before}}^V = \Delta d / d_{\text{before}}^V \quad (1)$$

Here, d_{before}^V and d_{after}^V are the Vickers indentation depths before and after heat treatment, respectively, and Δd is the difference between the depths. In our previous study,⁵⁾ a Knoop indenter

was used to measure RID because it induces less crack formation than a Vickers indenter. In the present study, however, a Vickers indenter was used to evaluate the load dependence of RID and crack initiation in the case of Vickers indentation. The relationship between the recovery after Knoop and Vickers indentation was described in our previous study.⁵⁾

3. Results and discussion

Photographs of indentations on the three glasses at a load of 100 gf are shown in Fig. 3. There are some differences in the shape and position of cracks among the glasses, as well as in the shape of indentation. In Glass C, which has the highest value of CR , no radials crack initiate. In Glass D, radial cracks initiate near some of the corners of the indentation, and the edge of the indentation are concave. In Glass G, radial cracks initiate at all corners of the indentation. Thus, even at the same indentation load, the number of initiating cracks and the shape of the indentation differ among the glass compositions.

Examples of AFM images of indentations in the glass samples before and after heat treatment are shown in Fig. 4. The recovery of the indentation diagonal during the heat treatment is very limited for all the glass samples. However, a remarked recovery of the opposite side (face-to-face) length of the indentation during the heat treatment was found in Glasses C and D, while the recovery of the opposite side length is small in Glass G. On the other hand, the annealing recovery of indentation depth is also significant in Glasses C and D. Examples of cross-section profiles measured with an AFM are shown in Fig. 5. In this figure, the depth recovery of Glass G is not distinct as compared with the other glasses. In all the glasses, the recovery of depth is the most remarked than those of diagonal length and opposite-side length. As for the soda-lime glass, it was also reported that the depth recovery was the largest among the annealing recoveries of diagonal length, opposite-side length, and depth.¹¹⁾ Therefore,

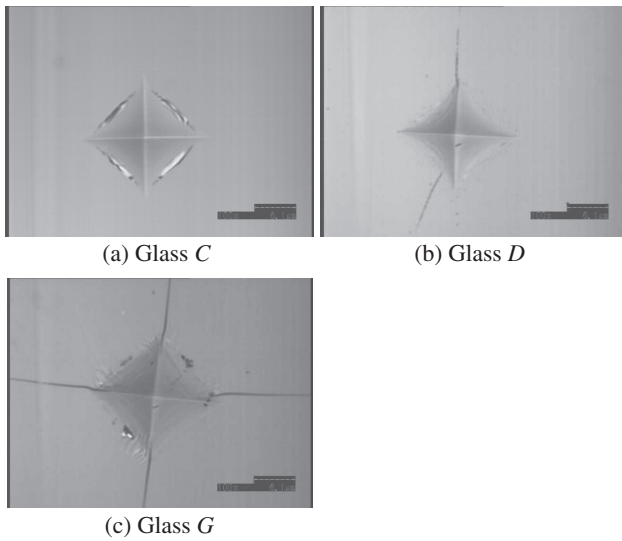


Fig. 3. Microscopic images of indentations at a load of 100 gf: (a) Glass C, (b) Glass D, (c) Glass G. The width of the images is 45 μm.

RID would be representative of the annealing recovery of indentation, and be one of the measures of the contribution of the densification under a Vickers indenter. Effects of indenter geometry of indentation recovery will be discussed later.

The indentation diagonal and *RID* for various applied loads are shown in **Table 2**, and the relationship between *RID* and the applied load is shown in **Fig. 6**. For Glasses C and D, the *RID* decreases with increasing applied load, similar to the results of Yoshida et al.⁶⁾ Note that Glasses C and D have almost the same value of *RID* at loads of up to 20 gf. However, *RID* for Glass D decreases more rapidly with increasing load than that for Glass C. Glass C has the largest value of *RID* at 200 gf. On the other hand, *RID* for Glass G is smaller than that for the other glasses at every indentation load.

Densification decreases the residual stress beneath the indentation.¹²⁾ Lawn et al.¹³⁾ proposed a method of estimating the residual stress using a simple cavity model. According to this model, the residual stress, σ_{rs} , can be expressed as

$$\sigma_{rs} = K \cdot \Delta V_{pf} / V_{pz}. \tag{2}$$

Here, σ_{rs} is the estimated residual stress, K is the bulk modulus, ΔV_{pf} is the plastic flow volume, and V_{pz} is the volume of the plastic zone around the indentation. By modifying Eq. (2), the residual

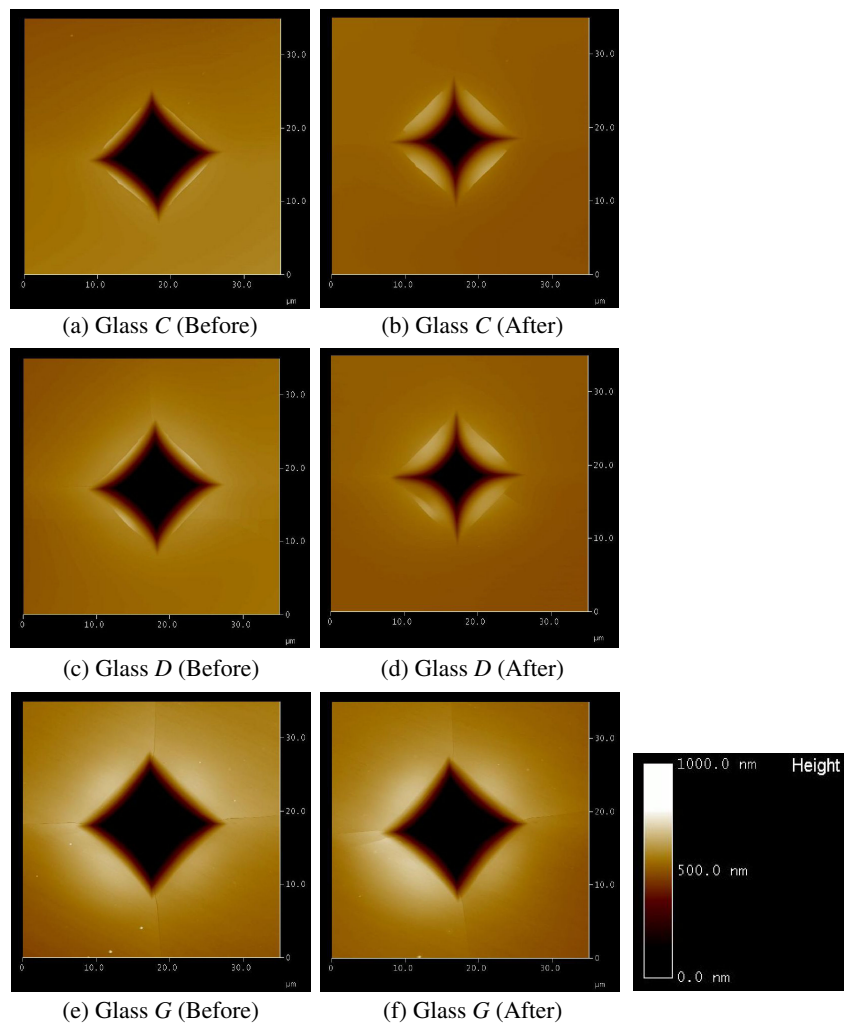


Fig. 4. (Color online) Examples of AFM images of Vickers indentations before and after heat treatment: Glass C [(a), (b)], Glass D [(c), (d)], and Glass G [(e), (f)]. The indentation load is 100 gf. The heat treatment temperature and holding time are $0.9 \times T_g$ (°C) and 2 h, respectively.

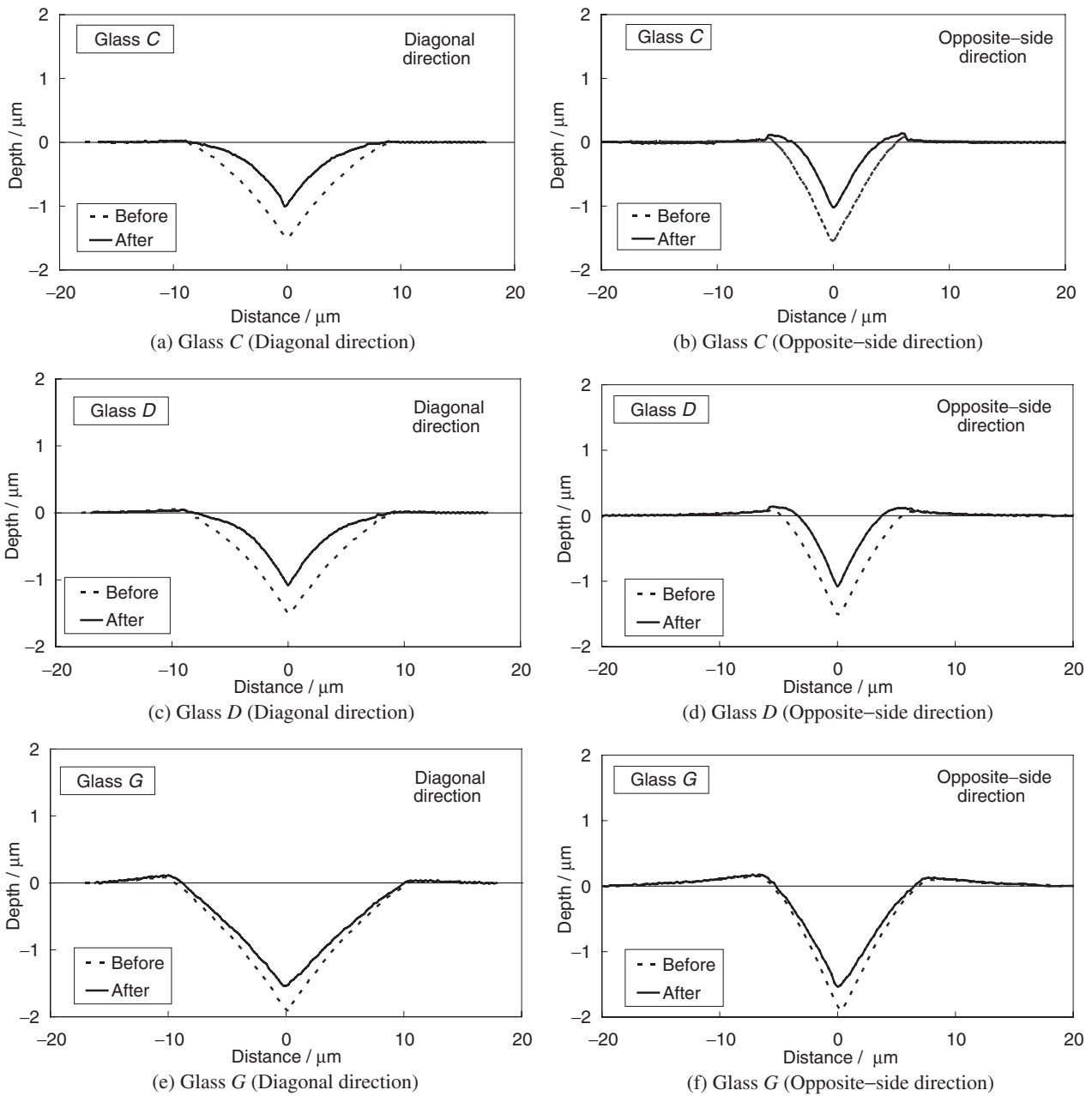


Fig. 5. Examples of cross-section profiles in diagonal direction and in opposite-side direction before and after heat treatment. Glass C [(a), (b)], Glass D [(c), (d)], and Glass G [(e), (f)]. The indentation load is 100 gf. The heat-treatment temperature and holding time is $0.9 \times T_g$ (°C) and 2 h, respectively.

stresses around the indentations of various commercial glasses were estimated in our previous study.⁵⁾ Yoffe¹⁴⁾ assumed that the plastic zone has a hemispherical shape with a diameter equal to the diagonal length of the Vickers indentation. If the indentation diagonal is $2a$, V_{pz} can be expressed by the following equation:

$$V_{pz} = (1/2) \cdot (4/3) \cdot \pi \cdot a^3 = 2.09 \cdot a^3. \quad (3)$$

The plastic flow volume, ΔV_{pf} , is assumed to equal the volume of the indentation after the heat treatment. Lawn et al.¹³⁾ assumed that ΔV_{pf} was equal to the volume of the indentation without any heat treatment. However, the part of the indentation volume attributed to densification contributes a little to stress generation because the densified part of the volume does not expand the plastic zone. Therefore, assuming that the diagonal length, $2a$, does not change during the heat treatment and that the projected

area of the Vickers indentation has a square shape, ΔV_{pf} can be approximated by

$$\Delta V_{pf} = (1/3) \cdot S \cdot d_{after}^V = (2/3) \cdot a^2 \cdot d_{after}^V. \quad (4)$$

Here, S is the projected area of the Vickers indentation and d_{after}^V is the Vickers indentation depth after the heat treatment.

By substituting Eqs. (3) and (4) into Eq. (2), the residual stress is expressed as

$$\sigma_{rs} = 0.319 \cdot K \cdot d_{after}^V/a. \quad (5)$$

It is assumed that the estimated residual stress is constant over the semi-sphere surface plastic zone. Although this cavity model is too simple to estimate the stress distribution around the indentation, it would be possible to evaluate the load and compositional dependences of the estimated residual stress

Table 2. Indentation depth before and after heat treatment (d_{before}^V and d_{after}^V), recovery of indentation depth (RID), and indentation diagonal length of Vickers indentation ($2a$) for each type of glass

Glass	Load/gf	$d_{\text{before}}^V/\mu\text{m}$	$d_{\text{after}}^V/\mu\text{m}$	RID	$2a/\mu\text{m}$
C	5	0.21	0.11	0.48	3.6
	10	0.35	0.20	0.43	4.9
	20	0.54	0.34	0.37	7.3
	50	0.97	0.63	0.35	12.6
	100	1.40	0.93	0.34	18.2
	200	2.21	1.60	0.28	26.7
D	5	0.21	0.11	0.48	3.4
	10	0.33	0.19	0.42	5.1
	20	0.56	0.34	0.39	7.6
	50	0.95	0.67	0.29	12.7
	100	1.38	1.05	0.24	18.5
	200	2.32	1.83	0.21	26.4
G	10	0.54	0.48	0.11	5.9
	100	2.20	2.05	0.07	19.7
	200	3.13	2.75	0.12	28.2

Experimental uncertainties are as follows. $2a$: $\pm 0.5 \mu\text{m}$, d_{before}^V and d_{after}^V : $\pm 0.03 \mu\text{m}$, RID : $\pm 3\%$.

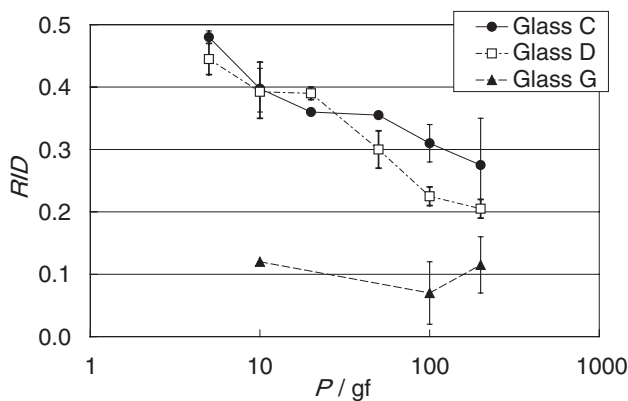


Fig. 6. Relationship between applied load (P) and RID .

qualitatively. The relationship between the calculated residual stress and the applied load is shown in Fig. 7. The residual stress increases with increasing load, not in a proportional manner but in a logarithmic manner.

A difference between the susceptibility to densification and that to plastic flow is considered to result in the load dependence of the residual stress. Densification is inelastic deformation with volume change while plastic flow is inelastic deformation with volume conservation. Densification proceeds through a process in which bond angles and the dihedral angle of the glass network are changed by external stress, while plastic flow proceeds through a process in which the bonds break and recombine sequentially. Since changing the bond angle requires less energy than bond breakage, the densification should occur at a lower stress than plastic flow. In previous papers,^{15,16} it was reported that the activation energy of the densification recovery process was much lower than that of viscous flow, which indicates that irreversible densification occurs more easily than plastic flow. On the other hand, a Vickers indenter has a finite tip radius, such as several hundred nanometers. This means that the maximum pressure under the indenter tip is not infinity but a finite value that increases with increasing load. The increased pressure results in a larger volume of plastic flow and a decrease in the

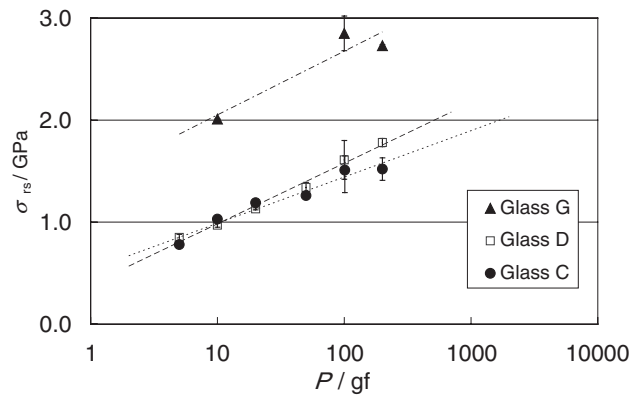


Fig. 7. Relationship between applied load (P) and estimated residual stress (σ_{rs}).

contribution of densification to the total deformation. With a further increase in the load, however, the effect of the tip radius should decrease and the contribution of densification should approach a constant value, which is determined by the shape of the indenter.

The packing density of ions in glass affects densification character among glasses. The packing density, the ratio of the total volume of constitutive ion spheres to the volume of the glass, can be calculated from the ionic radius estimated by the method of Pauling.¹⁷ The packing densities of Glasses C, D, and G were calculated to be 0.542, 0.544, and 0.561, respectively. Since a glass with a higher packing density has less free volume, Glass G exhibits the least densification. Since the packing density of Glass C is almost the same as that of Glass D, Glass C exhibits similar densification to Glass D.

The difference in the load dependence of the contribution of densification among glasses is considered to be related to the compositional variation of the relationship between pressure and the increase in density of glass. Rouxel et al.¹⁸ investigated the relationship between hydrostatic pressure and the increase in density of glass. With increasing applied hydrostatic pressure, the density of soda-lime glass does not increase until the hydrostatic pressure reaches a threshold pressure of about 10 GPa, above which it increases steeply. On the other hand, the density of B_2O_3 glass increases gradually above the threshold pressure of about 5 GPa. It is considered that such differences in the pressure dependence of hydrostatic densification result in differences in the distribution of densified region around an indentation, even if two glasses exhibit the same contribution of densification to deformation. In the case of a glass with a low threshold pressure, the wide distribution of the densified region is thought to form. Therefore, it is thought that the contribution of densification of glasses with a low threshold pressure does not decrease significantly with increasing load. Our previous study¹⁹ showed that RID increases with increasing amount of 3-coordinated boron and that almost all the boron in Glass C is 3-coordinated boron. The 3-coordinated boron in Glass C may be the origin of its low threshold pressure and the small slope of its load dependence of densification.

The large difference in CR among the glasses can be explained by the difference in the load dependence of densification or residual stress. It is assumed that cracks initiate at the load at which the residual stress around the indentation exceeds the critical stress required for crack initiation. The small difference in the slope of the load dependence of the residual stress between the glasses is thought to result in a large difference in the applied

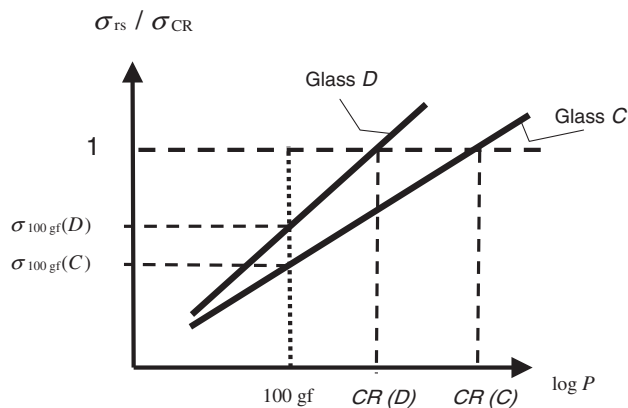


Fig. 8. Schematic diagram showing the relationship between the crack resistance and the critical stress for crack initiation. The horizontal axis is the logarithm of applied load (P), and the vertical axis is the normalized residual stress. The normalized residual stress is derived by dividing the residual stress (σ_{rs}) by the residual stress at the load corresponding to the crack resistance (σ_{CR}). $CR(C)$ and $CR(D)$ are the crack resistance of Glasses C and D , respectively. $\sigma_{100gf}(C)$ and $\sigma_{100gf}(D)$ are the normalized residual stresses at a load of 100 gf for Glasses C and D , respectively.

load at which the critical stress is generated. The reason for this is explained in Fig. 8. For simplification, only approximate lines for Glasses C and D are shown. In this figure, the horizontal axis is the logarithm of the applied load and the vertical axis is the residual stress normalized by the stress at a load corresponding to CR (σ_{CR}). [The approximate line in Fig. 5 for each glass is derived by the least-squares method, from which σ_{CR} for each glass can be estimated. The estimated values of σ_{CR} are 1.7 GPa for Glass D ($CR = 150$ gf) and 1.9 GPa for Glass C ($CR = 1200$ gf).] The normalized residual stresses at a load of 100 gf for Glasses C and D are also shown in Fig. 8 as $\sigma_{100gf}(C)$ and $\sigma_{100gf}(D)$, respectively. The value of CR , that is, $CR(C)$ or $CR(D)$ in Fig. 8, corresponds to the load at which the residual stress equals the critical stress ($\sigma_{rs}/\sigma_{CR} = 1$). Because the residual stress increases logarithmically with increasing applied load, the difference in crack resistance, $CR(C) - CR(D)$, is much larger than the difference in residual stress, $\sigma_{100gf}(C) - \sigma_{100gf}(D)$. Therefore, the difference in the load dependence of densification among the glass samples may result in the large difference in CR , which cannot be explained by the difference in other properties, such as K_{IC} , E , and H_v .

The difference in CR among the three glasses including Glass G cannot yet be explained quantitatively. The residual stress discussed in this paper is a highly simplified model. However, the actual stress distribution around indentations is more complex. As shown in Figs. 4 and 5, there is a large recovery of the opposite side length of the indentation, while there is little recovery of the indentation diagonal. This probably results from the variation of microscopic density of the glass under the indentation. The contribution of densification should be larger in the face of Vickers indentation than at the edge. As a result, a residual stress distribution should form in which the residual stress at the indentation corner is larger than that at the indentation edges. However, no theory has been proposed that can quantitatively describe the residual stress distribution around

an indentation. Therefore, direct measurement of the residual stress distribution is necessary to explain the difference in the stress distribution among the glass compositions. Moreover, stress distribution around an indentation varies dynamically during the process of indentation, which affects crack initiation behavior such as timing and position of initiating cracks. Therefore, the in situ observation of crack initiation during indentation and direct measurement of the residual stress distribution are future works that are expected to quantitatively clarify the differences in crack resistance.

4. Conclusion

The load dependence of densification was investigated for three commercial glass compositions. For the aluminoborosilicate glass (Glass C) and the soda-lime silicate glass (Glass D), the recovery of indentation depth (RID), which indicates the contribution of densification to the total deformation, decreases with increasing applied load. For the lead borosilicate glass (Glass G), RID is low throughout the range of applied loads. The estimated residual stress increases logarithmically with increasing applied load, and the slope of the load dependence of the stress is different among the glasses. This difference is thought to result in the large difference in crack resistance among the glasses.

References

- 1) M. Wada, H. Furukawa and K. Fujita, *Proc. of 10th International Congress on Glass*, **11**, 39–169 (1974).
- 2) B. R. Lawn and D. B. Marshall, *J. Am. Ceram. Soc.*, **62**, 347–350 (1979).
- 3) J. Sehgal and S. Ito, *J. Non-Cryst. Solids*, **253**, 126–132 (1999).
- 4) J. Sehgal, Y. Nakao, H. Takahashi and S. Ito, *J. Mater. Sci. Lett.*, **14**, 167–169 (1995).
- 5) Y. Kato, H. Yamazaki, S. Yoshida and J. Matsuoka, *J. Non-Cryst. Solids*, **356**, 1768–1773 (2010).
- 6) S. Yoshida, J.-C. Sangleboeuf and T. Rouxel, *Int. J. Mater. Res.*, **98**, 360–364 (2007).
- 7) J. E. Neely and J. D. Mackenzie, *J. Mater. Sci.*, **3**, 603–609 (1968).
- 8) S. Yoshida, S. Isono, J. Matsuoka and N. Soga, *J. Am. Ceram. Soc.*, **84**, 2141–2143 (2001).
- 9) S. Yoshida, J.-C. Sangleboeuf and T. Rouxel, *J. Mater. Res.*, **20**, 3404–3412 (2005).
- 10) J. D. Mackenzie, *J. Am. Ceram. Soc.*, **46**, 470–476 (1963).
- 11) H. Sawasato, S. Yoshida, T. Sugawara, Y. Miura and J. Matsuoka, *J. Ceram. Soc. Japan*, **116**, 864–868 (2008).
- 12) R. F. Cook and G. M. Pharr, *J. Am. Ceram. Soc.*, **73**, 787–817 (1990).
- 13) B. R. Lawn, A. G. Evans and D. B. Marshall, *J. Am. Ceram. Soc.*, **63**, 574–581 (1980).
- 14) E. H. Yoffe, *Philos. Mag. A*, **46**, 617–628 (1982).
- 15) M. Tashiro, S. Sakka and T. Yamamoto, *Yogyo Kyokaishi*, **72**, 98–103 (1964) [in Japanese].
- 16) J. Matsuoka, M. Sumita, M. Numaguchi, S. Yoshida and N. Soga, *J. Non-Cryst. Solids*, **349**, 185–188 (2004).
- 17) L. Pauling, “The Nature of the Chemical Bond and the Structure of Molecules and Crystals,” 2nd ed., Cornell University Press, Ithaca, N.Y. (1940).
- 18) T. Rouxel, H. Ji, V. Keryvin, T. Hammouda and S. Yoshida, *Adv. Mater. Res.*, **39–40**, 137–146 (2008).
- 19) Y. Kato, H. Yamazaki, Y. Kubo, S. Yoshida, J. Matsuoka and T. Akai, *J. Ceram. Soc. Japan*, **118**, 792–798 (2010).